

# ALMA polarimetric studies of rotating jet/disk systems

F. Bacciotti, J.M. Girart, M. Padovani, L. Podio, R. Paladino, L. Testi, E. Bianchi, D. Galli, C. Codella, D. Coffey, C. Favre and D. Fedele

**Abstract** We have recently obtained polarimetric data at mm wavelengths with ALMA for the young systems DG Tau and CW Tau, for which the rotation properties of jet and disk have been investigated in previous high angular resolution studies. The motivation was to test the models of magneto-centrifugal launch of jets via the determination of the magnetic configuration at the disk surface. The analysis of these data, however, reveals that self-scattering of dust thermal radiation dominates the polarization pattern. It is shown that even if no information on the magnetic field can be derived in this case, the polarization data are a powerful tool for the diagnostics of the properties and the evolution of dust in protoplanetary disks.

---

Bacciotti, F.

Istituto Nazionale di Astrofisica - Osservatorio Astrofisico di Arcetri, Largo Enrico Fermi, 5, I-50125 Firenze, Italy e-mail: [fran@arcetri.astro.it](mailto:fran@arcetri.astro.it)

Girart, J.M.,

Institut de Ciències de l'Espai (ICE, CSIC), Can Magrans, s/n, E-08193 Cerdanyola del Valles, Catalonia

Paladino R.,

Istituto Nazionale di Astrofisica - Istituto di Radioastronomia Via P. Gobetti, 101 40129 Bologna, Italy

Testi, L.,

European Southern Observatory, Karl-Schwarzschild-Strasse 2, 85748 Garching bei München, Germany

Bianchi, E.,

Institut de Planétologie et d'Astrophysique de Grenoble (IPAG) Université Grenoble Alpes, CS 40700, 38058 Grenoble Cédex 9, France

Padovani, M. Podio, L., Galli, D., Codella, C. Favre, F. Fedele, D.

Istituto Nazionale di Astrofisica - Osservatorio Astrofisico di Arcetri, Largo Enrico Fermi, 5, I-50125 Firenze, Italy

Coffey, D.,

School of Physics, University College Dublin, Belfield, Dublin 4, Ireland

## 1 Introduction

The process of formation of stars and planets is one of the most intriguing topics in current astrophysics. In recent years, high angular resolution studies like the ones conducted with the Hubble Space Telescope (HST) and the Atacama Large Millimeter/submillimeter Array (ALMA) have allowed us to advance significantly in the knowledge of protoplanetary disks and associated outflows. In particular, the sensitivity of ALMA allowed us to study the physical properties of young systems with an unprecedented combination of spectral and spatial resolution. One of the principal aims of such studies is to correctly set the initial conditions for planet formation.

In this context, the determination of the disk magnetic configuration is of particular interest, as magnetic fields may be responsible for the extraction of the excess of angular momentum from the system. This can occur via magneto-rotational instabilities generating an effective viscosity for horizontal transport [6]. Such instabilities, however, have proven to be ineffective for disk realistic conditions [5]. Alternatively, protostellar jets generated by magneto-centrifugal acceleration can transport angular momentum vertically along the ordered strong magnetic field attached to the star and the disk ([21, 9]). Magneto-centrifugal winds can originate from the star ('stellar winds'), the disk co-rotation radius ('X-winds') or from a wider range of disk radii (extended 'disk winds'). In any case proto-planetary disks are expected to be strongly magnetized, which would have fundamental implications for planetary formation and migration models [27].

The increase in sensitivity in mm-wave polarimetry has opened a new possibility to investigate the disk properties, and in particular the magnetic configuration. Polarimetry, in fact, has long been believed to provide the orientation of magnetic field lines, as non-spherical dust grains tend to align with their short axis perpendicular to the direction of the magnetic field ('grain alignment'), giving rise to linear polarization of the emission [2].

Polarization, however, can also arise from self-scattering of the thermal emission of dust grains of size of the order of the radiation wavelength. In this case the models show that the polarization direction is parallel to the minor axis for inclined disks [29, 17].

A third effect producing polarized emission is the alignment of non-spherical grains with an anisotropic radiation field. For a centrally illuminated disk, the linear polarization would present for this mechanism a circular pattern centred on the source [25].

The first studies on protostellar envelopes allowed the identification of large-scale hourglass-shaped and twisted patterns consistent with the winding-up of magnetic field lines due to the rotation of the envelope [10, 22]. Subsequent studies at moderate resolution reported detections of polarized emission on protostellar discs (e.g. [23, 16]) but in none of these cases the polarization structure showed a clear relationship with the expected magnetic configuration. More recently, the inner disk scales have been reached thanks to the advent of ALMA. Maps of the polarization of the dust emission have been derived for various targets, with resolution down to  $0.''1 - 0.''2$  (12 - 15 AU in nearby forming systems). A polarisation level of 0.5 - 2% can

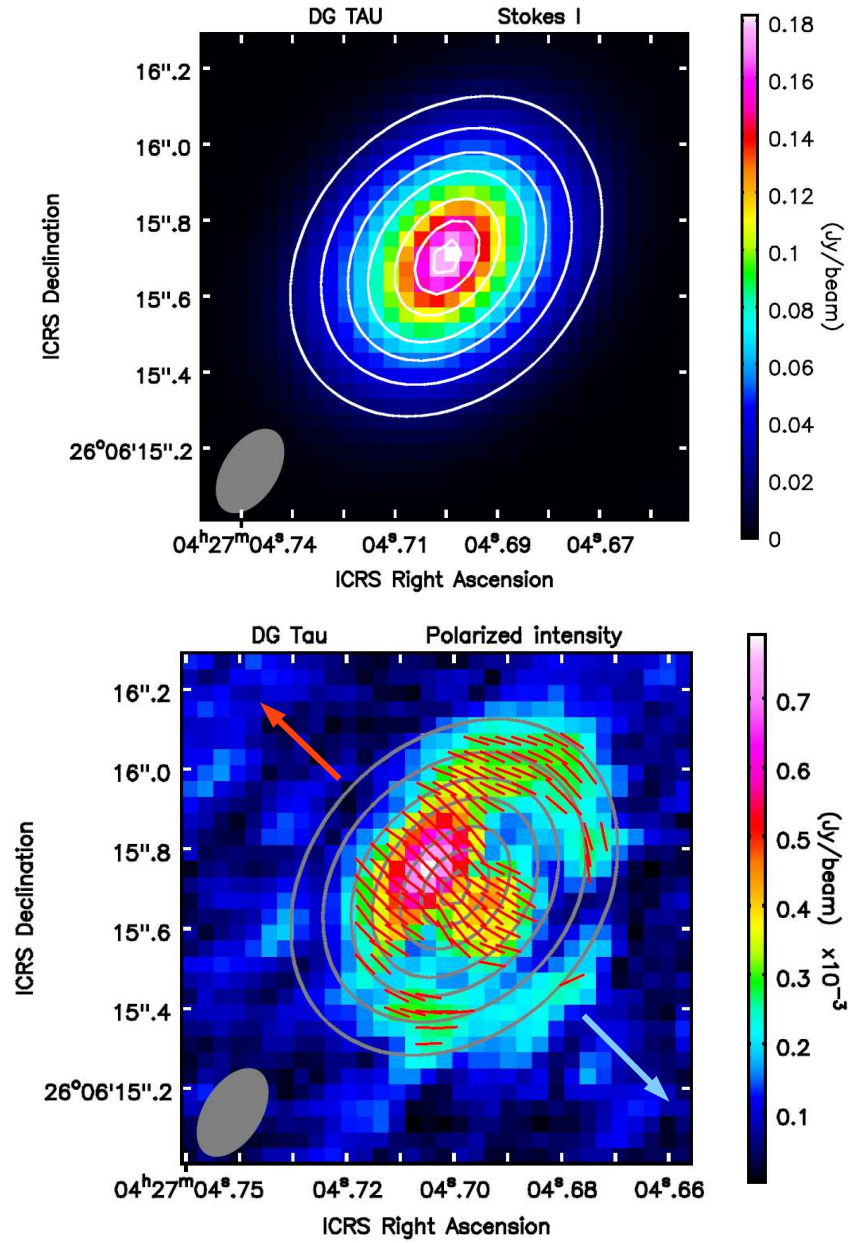


**Fig. 1** *Top* Total emission map at  $870 \mu\text{m}$  in the disks around DG Tau. Contour levels are  $[0.1, 0.2, 0.3, 0.4, 0.6, 0.8, 0.95] \times \text{peak value}$ , which is  $182.4 \text{ mJy beam}^{-1}$  for DG Tau. *Bottom* Linearly polarized intensity  $P$ . Contours are as in top panel and the Polarization angle is indicated with vector bars. The arrows indicate the jet orientation, with the disk near-side on the same side of the red arrow. As discussed in Sect.3, the evident asymmetry of the polarized intensity indicates a flared geometry for the disk.

easily be detected over the relevant regions of the disk with the expected ALMA sensitivity. These studies show that all the mechanisms mentioned above can produce polarization, but dust self-scattering appears to be dominant [24, 17, 18, 11, 13, 1].

In this framework, we have started a project to map the polarization properties of young evolved Class II systems with associated jets, as these systems offer fundamental observational constraints in both the cases in which scattering or magnetic properties dominate the polarized emission. In particular, we are interested in the sources for which the rotation kinematics of both the jet and the disk has been studied. The determination of the magnetic configuration for these targets can constitute the ultimate proof of the validity of the magneto-centrifugal mechanism for the launch of jets, which can realize the extraction of the excess angular momentum.

Following this line of research we selected and recently observed with ALMA the Class II sources DG Tau and CW Tau. These targets have been the subject of numerous studies in the past, both for their disks and their collimated jets [14, 19, 3, 12]. The two sources are nearby ( $d \sim 140$  pc), free of their parental envelope, are oriented favourably for polarization measurements and their dust emission is sufficiently strong. Importantly, the known kinematics of the jets and disks allows one to identify immediately the near-side of the disks and to give constraints on the expected magnetic configuration.

Despite our expectations, the observed polarization (shown in Sect. 2) does not seem to convey a simple interpretation in terms of an ordered magnetic structure. Instead, the results are fully consistent with self-scattering of the dust emission (see discussion in Sect. 3). This allows us to derive from the polarization measurements new information on the size and distribution of dust grains in the disk [4].

## 2 Polarized emission from DG Tau and CW Tau

In the following we illustrate the main features emerged from the polarimetric observations of DG Tau and CW Tau. More details can be found in [4].

The two targets were observed in full polarization mode in July 2017 within the ALMA Cycle 3 in Band 7 ( $870 \mu\text{m}$ ). The configuration of the interferometer for these observations included 40 antennas, giving an angular resolution of about  $0.''2$ . The datasets were reduced and analysed with the Common Astronomical Software Application (CASA) software.

From the Stokes I, U, Q maps we obtain the linear polarization intensity,  $P = \sqrt{Q^2 + U^2}$ , the linear polarization fraction,  $p = P/I$ , and the polarization angle,  $\chi = 0.5 \arctan(U/Q)$ , i.e. the direction of polarization of the electric field.

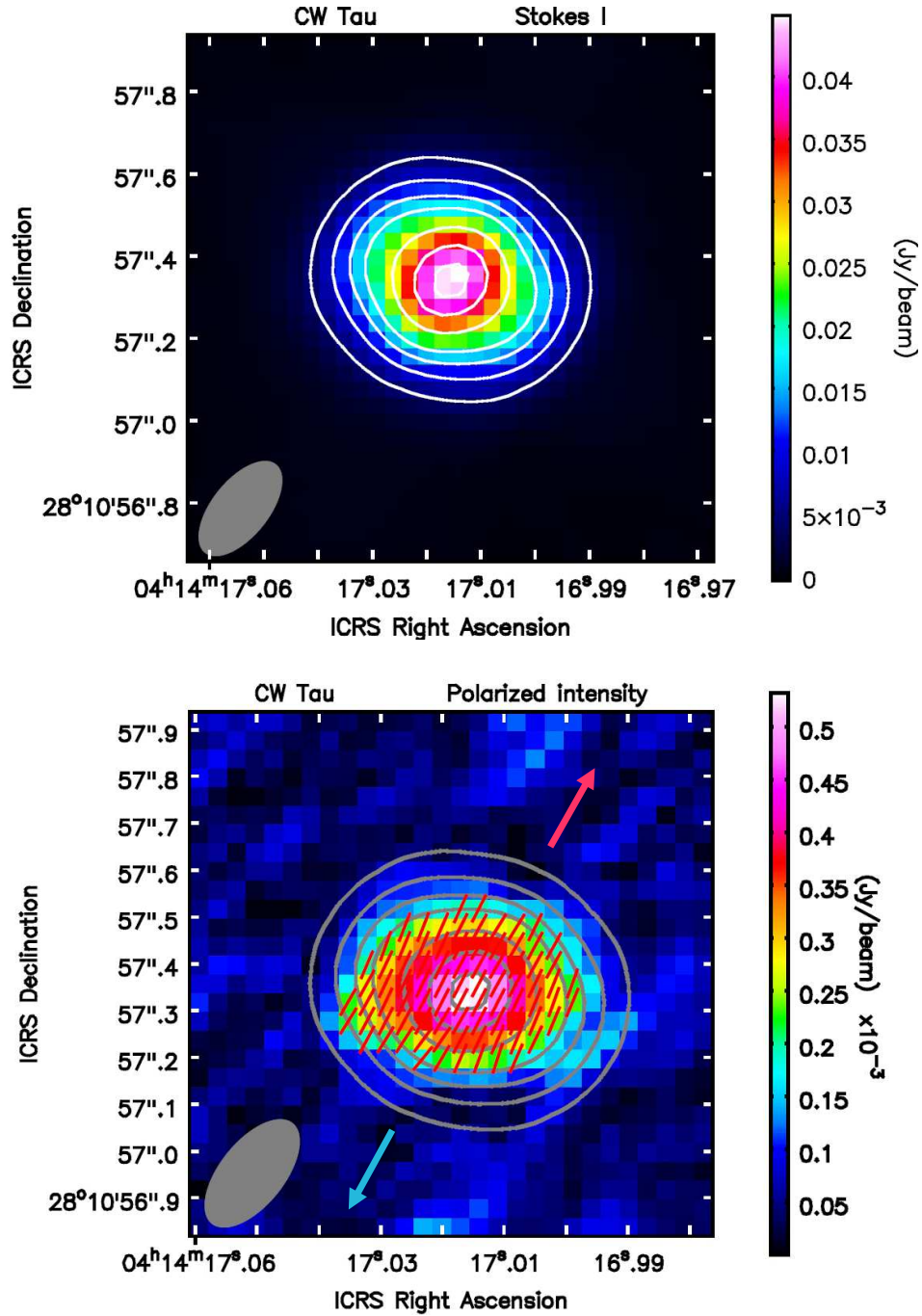


**Fig. 2** *Top* Total emission map at  $870 \mu\text{m}$  in the disks around CW Tau. Contour levels are  $[0.1, 0.2, 0.3, 0.4, 0.6, 0.8, 0.95] \times$  peak value, which is  $44.9 \text{ mJy beam}^{-1}$  for CW Tau. *Bottom* Linearly polarized intensity  $P$ . Contours are as in top panel. polarization angle,  $\chi$ , is indicated with fixed-length vector bars. The arrows follow the jet orientation. Disk near-side lies towards the receding jet lobe (red arrow). The central symmetry of the polarized intensity suggests a geometrically thin disk (see Sect.3).

## 2.1 DG Tau

The case of DG Tau is illustrated in Figure 1. The integrated flux is  $880.2 \pm 9.4$  mJy, with peak intensity of  $182.4 \pm 1.4$  mJy beam<sup>-1</sup>. The FWHM along the major and minor axis are  $0.''45$  and  $0.''36$ , respectively. These values imply  $i_{\text{disk}} \sim 37^\circ$ , while the measured disk PA is  $135.4^\circ \pm 2.5^\circ$ , almost perpendicular to  $\text{PA}_{\text{jet}} = 46^\circ$ .

The polarization properties of DG Tau are illustrated in the bottom panel of Figure 1. The near-side of the disk is brighter in polarized intensity, with the peak emission on the minor axis, displaced by  $\sim 0.''07$  from the photocenter of the total intensity. This feature, observed here for the first time in a disk around a low mass star, indicates that the disk has a flared geometry [29]. In the outer disk region, between  $0.''3$  and  $0.''5$  from the source, the polarized emission is distributed in a belt-like structure of lower intensity. The polarization vectors are nearly aligned with the disk minor axis in the central region, while they change orientation and become more azimuthal beyond  $0.''3$ . The linear polarization fraction (not shown) reflects the distribution of the polarized intensity. Averaging over the whole disk area one finds  $p = 0.41 \pm 0.17\%$ .

## 2.2 CW Tau

Figure 2, top panel, illustrates the total intensity of the  $870 \mu\text{m}$  continuum emission in CW Tau. For CW Tau, the integrated flux is  $145.1 \pm 1.4$  mJy, with peak intensity of  $44.9 \pm 0.3$  mJy beam<sup>-1</sup>. The FWHM along the major and minor axis is  $0.''35$  and  $0.''18$  respectively. From these values, we estimate a disk inclination  $i_{\text{disk}}$  with respect to the line of sight of  $\sim 59^\circ$ . The disk PA is  $60.7^\circ \pm 1.9^\circ$ , almost perpendicular to the jet  $\text{PA}_{\text{jet}} = -29^\circ$ .

The bottom panel of Figure 2 provides the map of the linearly polarized intensity  $P$ . This is centrally peaked and does not show any significant asymmetry. The polarization vectors are very well aligned along the minor axis of the disk. The polarization fraction,  $p$ , turns out to be almost constant in the disk central region of the disk, and it is on average  $1.15 \pm 0.26\%$ .

## 3 Dust properties derived from polarization measurements

The observed polarization properties can be explained in both sources in terms of self-scattering of the thermal dust emission [15, 29]. This is in agreement with the findings in other protoplanetary disks [17, 11, 13]. If self-scattering dominates the polarization, no information can be gathered on the orientation of the magnetic field. This unfortunate occurrence, however, is partly compensated by the fact that the comparison of the observed maps and the predictions of the models for self-scattering

give constraints on the size of the dust population of particles and on the geometry of the disk.

### 3.1 Grain Size

The analysis in [15] indicates that the maximum grain size contributing to polarization from self-scattering at a given wavelength,  $\lambda$ , is comparable to  $\lambda/2\pi$ . This implies a distribution peaked around  $140 \mu\text{m}$  in our case. Further constraints can come from the diagnostic diagrams that correlate grain size, wavelength and polarization fraction, as investigated, e.g. in [17]. Using our values of the average polarization fraction and the diagrams in this work we estimate that the maximum grain size giving rise to the observed polarization is in the range  $50 - 70 \mu\text{m}$  for DG Tau and about  $100 \mu\text{m}$  for CW Tau (see Fig. 3).

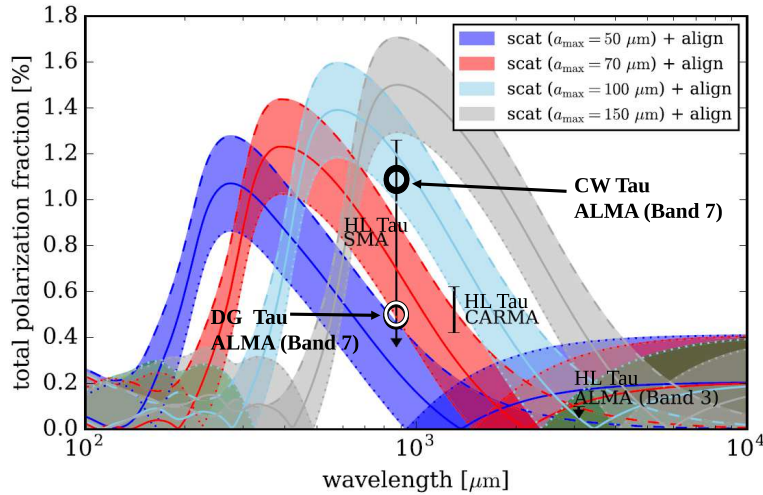


**Fig. 3** Diagnostics of grain size using a diagram adapted from [17]. The vertical bars refer to past observations for the disk around HL Tau with various interferometers. Our observations, performed at  $870 \mu\text{m}$  in ALMA Band 7, are indicated by the black and white circles. Their position corresponds to the average polarization fraction we measured for CW Tau and DG Tau, respectively. The average grain size turns out to be larger for CW Tau (about  $100 \mu\text{m}$ ) than for DG Tau ( $50 - 70 \mu\text{m}$ ).

### 3.2 *Grain settling toward the disk midplane*

In CW Tau, the distribution of the polarized intensity is symmetric, and polarization vectors are nearly parallel to the minor axis, with no curvature toward the outer disk. Since the disk around CW tau is reported to be optically thick by [19], the polarization models indicate that the observed features are consistent with self-scattering from a geometrically thin disk. Thus our observations indicate that the relatively larger grains in CW tau (see Section above) are more settled close to the disk midplane.

On the contrary, in DG Tau the polarization angle alignment is accompanied by an asymmetry in polarization intensity. This combination is consistent with the expectations of models of self-scattering in disks of intermediate or high optical depth, and with a finite angular thickness [29]. The disk is moderately optically thick according to [14], and the polarization maps are in agreement with the model expectations of [29]. Thus the observed asymmetry indicates that the scattering grains have not yet settled to the midplane.

### 3.3 *Hints for substructures in DG Tau ?*

We now consider the outer region of the DG Tau disk, i.e. beyond  $0.''3$  from the source. The bottom panel of Figure 1 shows structures in the polarized emission which do not correspond to any feature in the total intensity at the same resolution. In addition, a change in the orientation of the polarization pattern is observed. A possible explanation may come from a drop in the optical depth at  $0.''3$  from the star, corresponding to about 45 au at the distance of the system. This may imply that there is a substructure in the disk density at this location, like a gap or a ring, not revealed in the total emission (see discussion in [4]). The nature of such a structure has still to be revealed, and will require higher angular resolution observations. We anticipate, however, that a recent study in the emission of molecular lines has revealed a ring in the emission of formaldehyde (H<sub>2</sub>CO) whose inner border is at  $0.''3$  from the star, coincident with the change in the polarization properties [20]. Thus it appears that polarization maps nicely complement the investigations in total emission.

## 4 Conclusions

The ALMA observations of disks are providing new and precious information for the understanding of the formation of planets around young stars. In particular, the window opened recently by polarimetric capabilities allows us to set important constraints on the distribution and early evolution of the dust component of disks. As other systems recently observed, DG Tau and CW Tau show polarization properties at  $870 \mu\text{m}$  dominated by self-scattering of the dust thermal emission. Overall, DG



Tau appears to be in a less evolved state than CW Tau. In addition, structural peculiarities are revealed by the polarized emission. Our analysis thus indicates that polarimetry will be a powerful tool in the studies of the evolution of protoplanetary disks.

**Acknowledgements** FB wishes to dedicate this work to the loving memory of her mother-in-law Giovanna (Janet) Pesenti. FB also wish thanks the editors for their understanding in a difficult time. Support is acknowledged from the project EU-FP7-JETSET (MRTN-CT-2004-005592).

## References

1. Alves, F. O., Girart, J. M., Padovani, M., et al. *Astron. Astrophys.*, **616**, A56 (2018)
2. Andersson, B.-G., Lazarian, A., Vaillancourt, J. E. *Ann. Rev. Astron. Astrophys.*, **53**, 501 (2015)
3. Bacciotti, F., Ray, T. P., Mundt, R., Eisloffel, J., Solf, J. *Astroph. J.* **576**, 222 (2002)
4. Bacciotti, F., Girart, J. M., Padovani, M., et al. *Astroph. J. Lett.* **865**, L12 (2018)
5. Bai, X.-N., & Stone, J. M. *Astroph. J.* **769**, 76 (2013)
6. Balbus, S. A., & Hawley, J. F. *Astroph. J.* **376**, 214 (1991)
7. Blandford, R. D., Payne, D. G. *Mon. Not. Roy. Astr. Soc.* **199**, 883 (1982)
8. Coffey, D., Bacciotti, F., Ray, T. P., Eisloffel, J. and Woitas, J. *Astroph. J.* **663**, 350 (2007)
9. Frank, A., Ray, T. P., Cabrit, S., et al. in *Protostars and Planets VI*, ed. by H.Beuther, R.S. Klessen, C.P. Dullemond, and T.Henning, University of Arizona Press, Tucson, p.451–474 (2014)
10. Girart, J. M., Rao, R., Marrone, D. P. *Science*, **313**, 812 (2006)
11. Girart, J. M., Fernández-López, M., Li, Z.-Y., et al. *Astroph. J. Lett.* **856**, L27 (2018)
12. Hartigan, P., Edwards, S., & Pierson, R. *Astroph. J.* **609**, 261 (2004)
13. Hull, C. L. H., Yang, H., Li, Z.-Y., et al. *Astroph. J.* **860**, 82 (2018)
14. Isella, A., Carpenter, J. M., Sargent, A. I. *Astroph. J.* **714**, 1746 (2010)
15. Kataoka, A., Muto, T., Momose, M., et al. *Astroph. J.* **809**, 78 (2015)
16. Kataoka, A., Tsukagoshi, T., Momose, M., et al., *Astroph. J.* **831**, L12 (2016)
17. Kataoka, A., Tsukagoshi, T., Pohl, A., et al. *Astroph. J. Lett.* **844**, L5 (2017)
18. Lee, C.-F., Li, Z.-Y., Ching, T.-C., Lai, S.-P., Yang, H. *Astroph. J.* **854**, 56 (2018)
19. Piétu, V., Guilloteau, S., Di Folco, E., Dutrey, A., Boehler, Y. *Astron. Astrophys.* **564**, A95 (2018)
20. Podio, L. et al., *Astron. Astrophys. Lett.*, submitted
21. Pudritz, R. E., Ouyed, R., Fendt, C., & Brandenburg, A. in *Protostars and Planets V*, ed by B. Reipurth, D. Jewitt, and K. Keil, University of Arizona Press, Tucson, p.277–294 (2007)
22. Rao, R., Girart, J. M., Marrone, D. P., Lai, S.-P., Schnee, S. *Astroph. J.* **707**, 921 (2009)
23. Rao, R., Girart, J. M., Lai, S.-P., Marrone, D. P. *Astroph. J. Lett.* **780**, L6 (2014)
24. Stephens, I. W., Yang, H., Li, Z.-Y., et al. *Astroph. J.* **851**, 55 (2017)
25. Tazaki, R., Lazarian, A., & Nomura, H. *Astroph. J.* **839**, 56 (2017)
26. Testi, L., Bacciotti, F., Sargent, A. I., Ray, T. P., Eisloffel, J. *Astron. Astrophys.* **394**, L31 (2002)
27. Turner, N. J., Fromang, S., Gammie, C., et al., in *Protostars and Planets VI*, ed. by H.Beuther, R.S. Klessen, C.P. Dullemond, and T.Henning, University of Arizona Press, Tucson, p.411–432 (2014)
28. Yang, H., Li, Z.-Y., Looney, L., Stephens, I. *Mon. Not. Roy. Astr. Soc.* **456**, 2794 (2016)
29. Yang, H., Li, Z.-Y., Looney, L. W., Girart, J. M., Stephens, I. W. *Mon. Not. Roy. Astr. Soc.* **472**, 373 (2017)